Chapter 14

Characterization of microbialites and microbial mats of the Laguna Negra hypersaline lake (Puna of Catamarca, Argentina)

Flavia J. Boidi[1], Cecilia Mlewski[1], Fernando J. Gomez[1],Emmanuelle Gerard[2]

[1]CICTERRA-Centro de Investigaciones en Ciencias de la Tierra, CONICET-UNC, Córdoba, Argentina
[2]Université de Paris, Institut de Physique du Globe de Paris, CNRS, UMR 7154, F-75238 Paris, France

14.1 Abstract

Microbial carbonates provide an invaluable tool to understand biogeochemical processes in aqueous systems, especially in lacustrine and marine environments. Lakes are strongly sensitive to climatically-driven environmental changes and microbialites have recently shown to provide a record of these changes. Unraveling physicochemical and microbiological controls on carbonates textures and geochemistry is necessary to correctly interpret these signals and the microbial biosphere record within sedimentary carbonates.

The Laguna Negra is a high-altitude hypersaline Andean lake (Puna of Catamarca, Argentina), where abundant carbonate precipitation takes place and makes this system an interesting example that preserves a spectrum of carbonate fabrics that reflect complex physical, chemical, and biological interactions. The extreme environmental conditions (high UV radiation, elevated salinity, and temperature extremes) make the Laguna Negra a good analogue to some Precambrian microbialites (e.g., Tumbiana Fm., Archean, Australia). In addition, the discovery of ancient evaporating playa-lake systems on Mars surface (e.g., ShalbatanaVallis, Noachian, Mars) highlights the potential of Laguna Negra to provide insight into biosignature preservation in similar environments. Given that microbial processes in the Laguna Negra can be studied with remarkable detail, this may provide insight into biosignature preservation in both, terrestrial and extraterrestrial settings.

14.2 Introduction

The Puna-Altiplano region (including northwest Argentina, north Chile and south Bolivia) has become an interesting region to study microbial mineralization processes. The convergence of factors such as extreme environmental conditions, particularly strong negative hydrological balance, favors the development of these mineralizing systems, and of extremophile microbial communities. This, together with a favorable local geology and geomorphology, facilitate the formation of closed lakes and groundwater springs which are saturated in minerals, including carbonates. Thus, a highly mineralizing setting together with physico-chemical and microbiological processes trigger carbonate precipitation and produce a set of diverse organo-sedimentary structures usually referred as microbialites (cf. Burne and Moore 1987). Some ofthe Puna-Altiplanomicrobialites resemble those observed in the ancient geological record, for example stromatolites, which are the oldest evidence of life on Earth (Allwood *et al* 2006). Thus, thesemicrobialites systems provide a unique opportunity to apply an integrated geobiological approach, to gain insight to understand microbial mineralization processes and biosignatures preservation.

The Laguna Negra (LN) is an interesting system that called our attention 10 years ago given the presence of an extensive plain with abundant carbonate precipitation (Figure 14.1).

The evaporative sedimentary environment, the diversity of microbial mat types and the combination of physico-chemical and microbial processes influencing carbonate precipitation and carbonates geochemistry makes this place an excellent natural laboratory that shows strong similarities with some ancient microbial mineralizing systems, including the Precambrian microbialites of the Tumbiana Formation (Australia, Buick 1992,Awramik and Buchheim 2009) and the Strelley Pool Chert Formation (Australia, Allwood *et al* 2006). Here some recent findings are summarized to discuss the combination of microbial and physicochemical processes involved in carbonate precipitation and microbialite formation.

Figure 14.1 Left: Location map of the study area (red square). Center: Panoramic view of the LN, the Stromatolite Belt (SB) and the Saline Plain. Right: Spatial zoning of the LNStromatolite Belt.

14.3 Geological and environmental setting

The LN is a shallow (≤2 m) hypersaline lake located at 4200 meters above sea-level with an area of ~8.63 km^2 and, as most lakes in the region, a strongly negative water balance. It is part of the Laguna Verde Complex, which is in northwest Argentine, at the southern end of the Puna Plateau (Catamarca province), a high-altitude plateau in the Andean region (Figure 14.1). The high-altitude, hot and dry climate combine to favor the precipitation of evaporites (halite, gypsum, calcite, etc) and set extreme conditions where microbial mats adapted to hypersalinity as well as high UV radiation influx develop.

The microbial mats distribution and carbonate precipitation are mostly spatially restricted to the region where groundwater springs mixes with the main lake, a region of ~0.3 km^2 that it is called the *Stromatolite Belt* (Gomez *et al* 2014). Geochemical modeling suggests that this water mixing increases the saturation state of carbonate minerals favoring abundant carbonate precipitation (Gomez *et al* 2014). The presence of microbial mats also influences carbonate precipitation processes, the resulting textures and geochemical signatures (Gomez *et al* 2018, Buongiorno *et al* 2018).

14.4 Microbialite spatial zoning in the Laguna Negra

The Stromatolite Belt presents three main distinct zones mostly defined by a combination of sedimentary environment, microbialite morphology, water depth and salinity:

Zone 1: a proximal belt that is colonized by salt-marsh grass in the region of freshwater input,
Zone 2: an intermediate zone consisting of microbial ponds that lack both oncolitic structures and mineralization,
Zone 3: the main belt of carbonate oncoidalmicrobialites and crusts. This zone can also be separated into four zones;**Zone 3A** where *laminar crusts* are common, **Zone 3B** with centimeter-scale *carbonate gravel aggregates* and **Zone 3C** where *oncoids* are primarily concentrated, and **Zone 3D** is represented mainly by peloidal to *micritic carbonate sediment*,

locally interlayered with gypsum or organic-rich laminae. The transition between Zones 3C and 3D is where *stromatolites* are typically represented, and these where not previously described by Gomez *et al* (2014) nor (2018).

14.6 Microbialites macro-morphologies

Previous work allowed to recognize and to characterize the different carbonate microbialites morphologies within the LN (Gomez *et al* 2014, Gomez *et al* 2018,Mlewski*et al* 2018, Buongiorno *et al* 2018). Three main types of macro-morphologies (at the decimeter-size scale) have been documented in the LN and here their main macroscopic features are summarized (Figures 14.2 to 14.6, and Table 1). For details about the different microbialites micro-textures see Table 1 (for a deeper analysis see Gomez *et al* 2014 and 2018, Mlewski*et al* 2018). These structures include *Laminar Crusts*, *Oncoids* and *Stromatolites*.

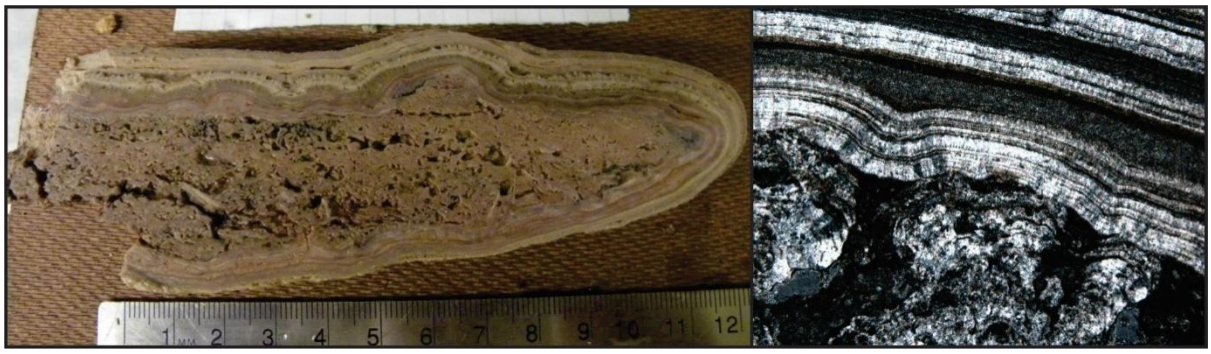

Figure 14.2 Polished slab (left) and thin-section (right) of the LN laminar crusts.

Laminar crusts: are present in the region that is better connected with the main lake, on the northwest side of the Stromatolite Belt. These are represented by millimeter to decimeter carbonate crusts encrusting volcanic rocks, carbonate sediments and other microbial structures as well as organic remains (e.g. flamingoes feathers) (Figure 14.2). These can have a patchy distribution or form laterally continuous crusts (at a meter scale), covering loose or cemented carbonate sediments (peloidal and nodular carbonates). Carbonate plates formed by laminar crusts can coalesce to form more complex structures and can have overgrowths and show different growth stages due to movement and rotation by currents or cryoturbation processes. Laminar crusts can also develop dome-shaped morphologies, occasionally showing concentric growth patterns (Figure 14.2). In addition, oriented and elongated structures are common, where these develop according to the main currents related to the prevailing winds (from north west to south east) (Figure 14.3). Although regular isopachous laminae (Figure 14.2) are the main building blocks of the laminar crusts (see details in Table 1), it worth mentioning that the wind-oriented structures, in cross-section, develop more complex micro-textures. These include columnar, shrub-like to dendritic and micro-stromatolite microfabrics, that resemble microbially-influenced structures but related to abiotic carbonate precipitation. These are formed by preferential growth where advective-diffusive flux provides calcium and carbonate ions (Figure 14.3), in an analogous way to silica and carbonate dendrites developed under unidirectional flow (see for example numerical models by Hawkins *et al* 2013 and 2014). These dendrite-shrubs-rich layers alternate with the previously described smooth laminar crusts.

Interpretation: Given the absence of microbial mats, and the macro-morphologies and micro-textures described (e.g. lamina regularity and degree of inheritance, lack of organic remains within the lamina,etc), these structures have been interpreted as predominantly chemically precipitated carbonates, triggered by oversaturation related to water mixing

(Gomez *et al* 2014), strong CO_2 degassing and evaporation (see Gomez *et al* 2014, Buongiorno *et al* 2018, Beeler *et al* in press).

Figure 14.3 Current-oriented structures observed in the Zone 3A. **a)** Hand-sample, **b)** Polished slab in cross-section. The white dotted line marks the location of the sediment-water interface during sampling. **c)** Closer view of the polished slab showing the complex micro-columnar to dendritic internal structure with preferential growth on the side affected by currents. The black arrows indicate the current transport direction. **d-e)** Thin-sections showing the micro-columnar to dendritic micritic to micro-spar-rich textures that alternate with more regular laminar, smooth isopachous laminae. **f)** On the left side panel, it can be seen the resulting modeled columnar to dendritic structures developed due to mineral precipitation under unidirectional flow, and on the right side an example of silica micro-columns and dendrites (both pictures taken from Hawkins *et al* 2013, 2014).

Oncoids: these are typically located in the central area of the Stromatolite Belt and are composed by concentrically laminated, centimeter to decimeter spheroidal structures (up to ~35 cm). Morphologically these are represented by discs, spheres and flattened domes that can coalesce to form more complex, composite structures (Figure 14.4). Oncoids grow by the accretion of smooth to irregular and overlapping laminae, showing lateral protrusions, typically formed at the water-sediment as well as air-water interface. External surface can be smooth or can show pillar-like to shrub-shaped millimeter scale protrusions and ornamentations (Figure 14.4), particularly on the side affected by wind and currents. Oncoid rotation, particularly by cryoturbation, is also common producing more complex overlapping overgrowths. Oncoids are typically associated with well-stratified pinkish to orange microbial mats (Figure 14.8) but can also be colonized by cyanobacteria-rich microbial mats (*Rivularia halophila*) (Mleswki*et al* 2018, Shalygin*et al* 2018) which produce a different set of carbonates micro-textures and lateral overgrowths (Table 1, see Gomez *et al* 2018 and Mlewski*et al* 2018 for details). Although oncoids are subspherical in shape, they can show asymmetric growth, occasionally expanded below the sediment-water interface, thus showing both *hydrogenetic* and *diagenetic* growth (above and below the sediment-water interface respectively) (Figure 14.5) in an analogous way to manganese nodules observed in the deep sea (Figure 14.5, right), being morphologically similar and suggesting similar diffusive-reactive processes involved in oncoids growth (Baker and Beaudoin 2013).

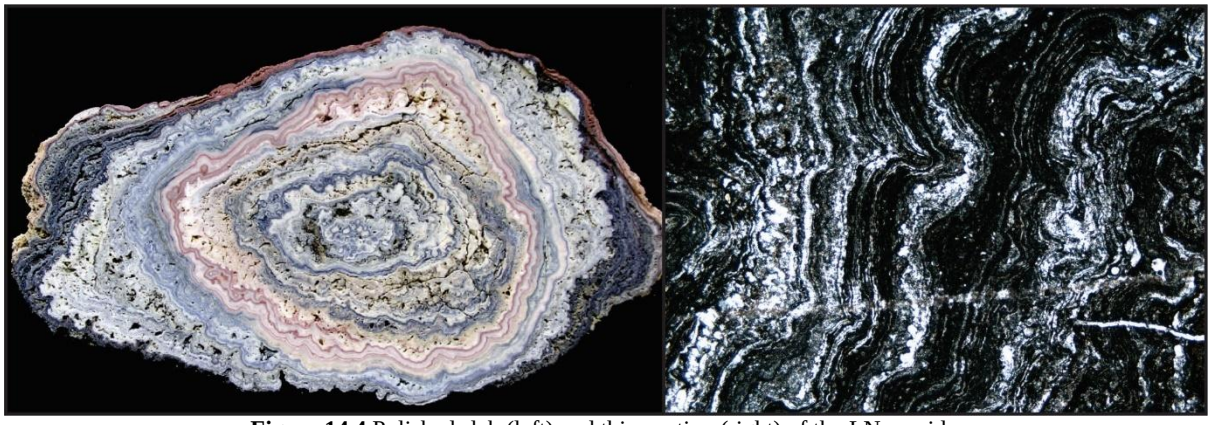

Figure 14.4 Polished slab (left) and thin-section (right) of the LNoncoids.

Interpretation: Given that oncoids are closely associated with microbial mats, the recorded morphologies and the diverse set of micro-textures observed in previous work (Table 1), these structures are interpreted as microbially influenced structures. The microbial influence is particularly observed in the development of microfabrics as well as the geochemical signatures preserved in the carbonates (Gomez *et al* 2014, Buongiorno *et al* 2018). Despite this, physicochemical processes (mostly water mixing, CO_2 degassing and evaporation) are also particularly important to trigger carbonate precipitation (Gomez *et al* 2014, 2018, Buongiorno *et al* 2018, Beeler *et al* in press). The observed differential growth patterns, where oncoids grow bigger in the diagenetic zone (below the sediment-water interface), suggests that at least in some cases growth rates are higher in the anoxic zones. This is probably related to the influence of anoxic microbial metabolisms (likes sulfate reduction) that are known to increase alkalinity and thus carbonate precipitation.

Figure 14.5- a) Carbonate oncoids of the Laguna Negra Stromatolite Belt where hydrogenetic and diagenetic growth zones are observed and marked by the sediment-water interface (white dotted lines). **b)** Manganese nodules with the same growth patters shown for comparative purposes and suggesting comparable growth mechanisms (from Baker and Beaudoin 2013).

Stromatolites: Stromatolites here represent centimeter to decimeter-scale laminated structures (up to 25 cm) that typically have a planar to columnar shape (Figure 14.6) that resemble classic stromatolites. These are observed on the east side of the Stromatolite Belt (transition between Zones 3C and D), associated to dark greenish to black microbial mats and biofilms and usually are encrusting previous structures (typically oncoids) (Figure 14.6), as

well as loose to cemented sediments and other carbonate crusts. The columnar structures are usually centimeter-size and represent mini-stromatolites (Figure 14.6). The main difference with oncoids and laminar structures is in the shape (planar to columnar) and in the micro-textures, predominantly irregular, crenulated micritic to micro-peloidal crusts that preserve abundant organic remains (Figure 14.6 and Table 1).

Interpretation: Given the crenulate and overlapping, irregularly shaped micrite-to micro-spar-rich laminae, which also preserve abundant organic remains, these are also interpreted as microbially influenced structures, as typically observed in other microbialites (Riding 2008). Since these structures are usually nucleated on oncoids (Figure 14.6), it suggests changes in growth patterns probably triggered by local environmental changes as well as in the microbial mat type.

Table 14.1 Summary of the main micro-textures preserved in the LNmicrobialites (for details see Gomez *et al* 2014, 2018, Mlewski*et al* 2018, Buongiorno *et al* 2018).

Microbialite Type	Microfabric Elements	Observations
Laminar Crusts - mm to cm thick laminated crusts forming patchy to laterally extensive pavements	Isopachous laminae	Microbial mats are typically absent. Remarkable regular isopachous lamina with high degree of inheritance during lamina accretion. This results in translation and gradual smoothing of surface morphology. Lamina composed by closely spaced acicular calcite crystals, individual laminae (50-100 µm thick) are separated by micrite isopahcous laminae (10-50 µm thick) composed by irregularly shaped anhedral to subhedral calcite crystals. Smaller scale lamination (≤ 5 µm) given by luminescence changes related to variable trace elements content.
Oncoids - cm- to dm-scale concentrically laminated discs, spheres and flattened domes	Alternating micritic and botryoidal laminae (cf. Gomez *et al* 2014).	Mostly developed in ponds with pinkish to orange stratified mats. Alternating micritic and botroidal lamina are usually irregular with variable thickness (50–500 µm thick). These are the most common lamina types in these structures. Micritic: represented by nanometer-scale spherical, globular, or spherulitic calcite (up to 300 nm) or more irregular globular to anhedral calcite. Botryoidal: individual or stacked micro-laminated botryoids (300 µm wide and 100 µm tall) or radial fibrous crystal bundles (50–100 µm wide 400–600 µm tall) associated with bacteria remains and diatom frustules.
	Locally microspar lamina with preserved *Rivularia*-like filaments	Laminae bearing *Rivularia*-like filaments: irregular laminae with tufted dark brown to yellowish vertically oriented filaments (diameter 15–20 µm) in micro-spar translucent carbonates. Filaments form a paintbrush-like (cf. Reitner*et al* 1996) palisade fabric. Alternates with micrite or botryoidal laminae.
	Whitish irregular granular laminae	White granular precipitates with the presence of diatom and forming irregular laminae alternating with other lamina types. It shows characteristic remarkably similar to the granular texture and diatom–bacteria aggregates observed in the stratified pinkish-orange microbial mats thus being a fossilized equivalent.
	Spar to microspar laminae with oriented pennate diatoms	Irregular and translucent microspar laminae, occasionally micritic. Parallel-oriented pennate diatom frustules. This has also been recorded during diatom blooming events in the areas where the pinkish-orange microbial mats are common.
Stromatolites - cm to dm-scale flat to columnar stromatolites	Micritic laminae	Within ponds where stromatolites are covered by dark green to grey colored biofilms. These mini-stromatolites are columnar at the cm-scale and usually encrusting previous oncoids. Micritic laminae are irregular (100-300 µm thick) and shows variably preserved organic remains (degraded coccoid clusters) which are evident by fluorescence under UV light microscopy.

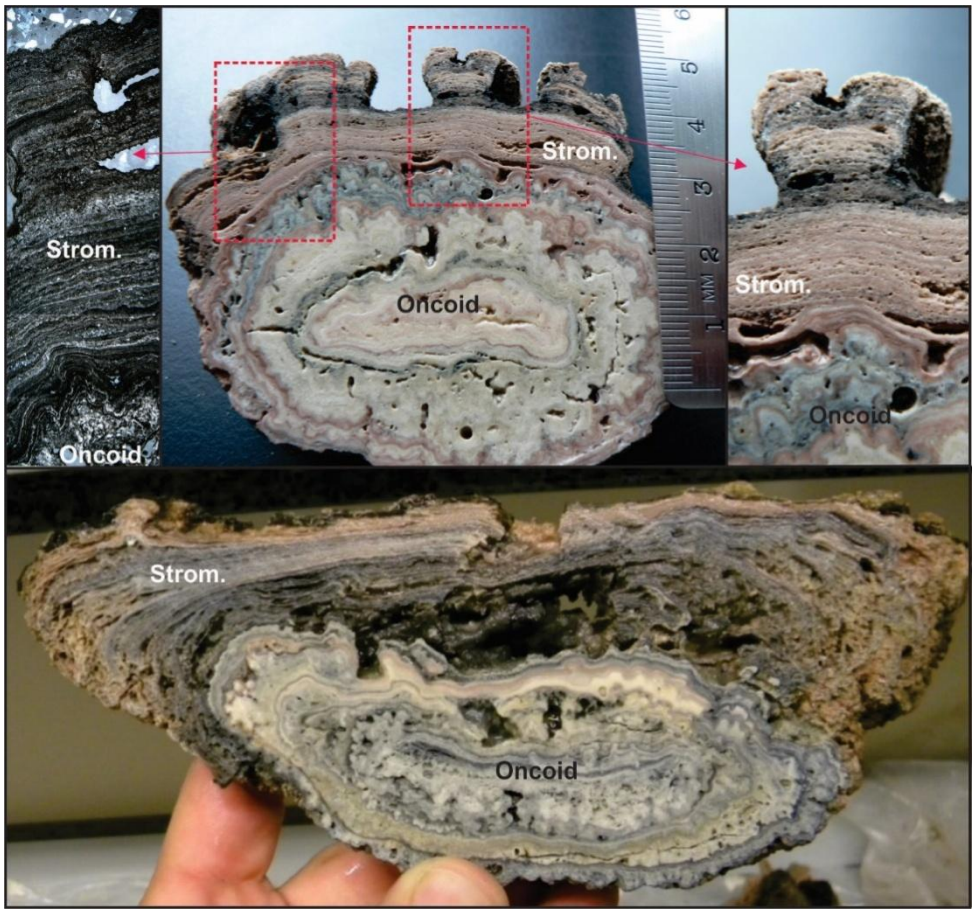

Figure 14.5 Well-laminated planar to mini-columnar stromatolite nucleated over an oncoidal structure showing concentric growth.

14.7 Stable isotopes of the Laguna Negra microbialites (Carbon and Oxygen)

Previous studies of $\delta^{13}C$ and $\delta^{18}O$ in the LN carbonates showed strong isotopic enrichment, particularly of the $\delta^{13}C$ of the carbonates reaching values up to 18‰ (Gomez *et al* 2014, Buongiorno *et al* 2018). This enrichment is similar to what has been observed in other saline lakes in the Puna-Altiplano region (Valero-Garces *et al* 1999, 2000). Figure 14.7 shows a cross-plot of the $\delta^{13}C$ and $\delta^{18}O$ showing covariation, as typically observed in closed lakes where evaporation and CO_2 degassing are important (Talbot 1990) usually following a Rayleigh distillation pattern (Valero-Garces *et al* 2000, Buongiorno *et al* 2018).

In addition to the covariation pattern, Buongiorno *et al* (2018) showed that both, $\delta^{13}C$ and $\delta^{18}O$ values decreased over time, that is when observed from the core to the outer edge of the oncoids and laminar crusts. These can show a change of up to 8‰ in $\delta^{13}C$ and 4‰ in $\delta^{18}O$ toward lower values. This was interpreted as due to progressive *freshening*, the increase in the influx of freshwater carrying a lighter isotope signal (for details see Buongiorno *et al* 2018). An increase in humidity between 2200-1800 years before present has been documented with different proxies, with an estimated increase of 15-20% (Boschetti*et al* 2007). This pattern towards lighter isotopes is less clear in the laminar crusts (when compared with the oncoids), given that in Zone 3A the mixing rate with groundwater is lower so the evaporation signal is stronger, as suggest heavier values in $\delta^{18}O$ of laminar crusts when compared with oncoids (Buongiorno *et al* 2018).

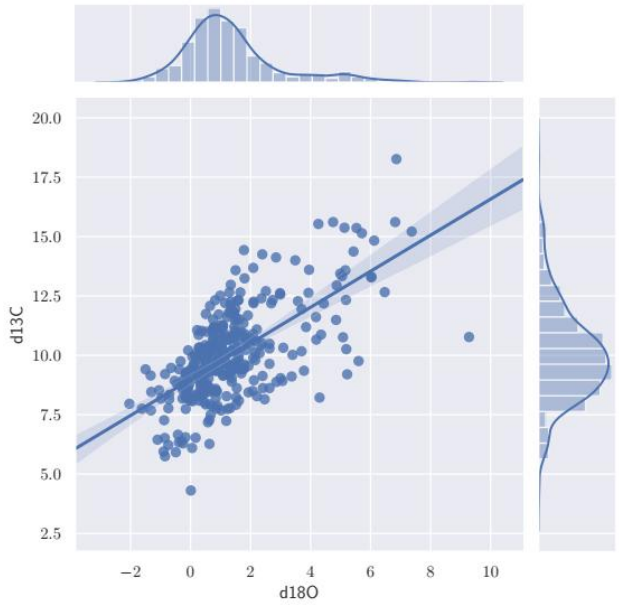

Figure 14.7 Cross-plot of the carbon and oxygen stable isotopes of the LNmicrobialites and laminar crusts compiled from those published by Gomez *et al* (2014) and Buongiorno *et al* (2018). The adjusted trend line is $\delta^{13}C=0.76*\delta^{18}O +8.9$ (R=0.65).

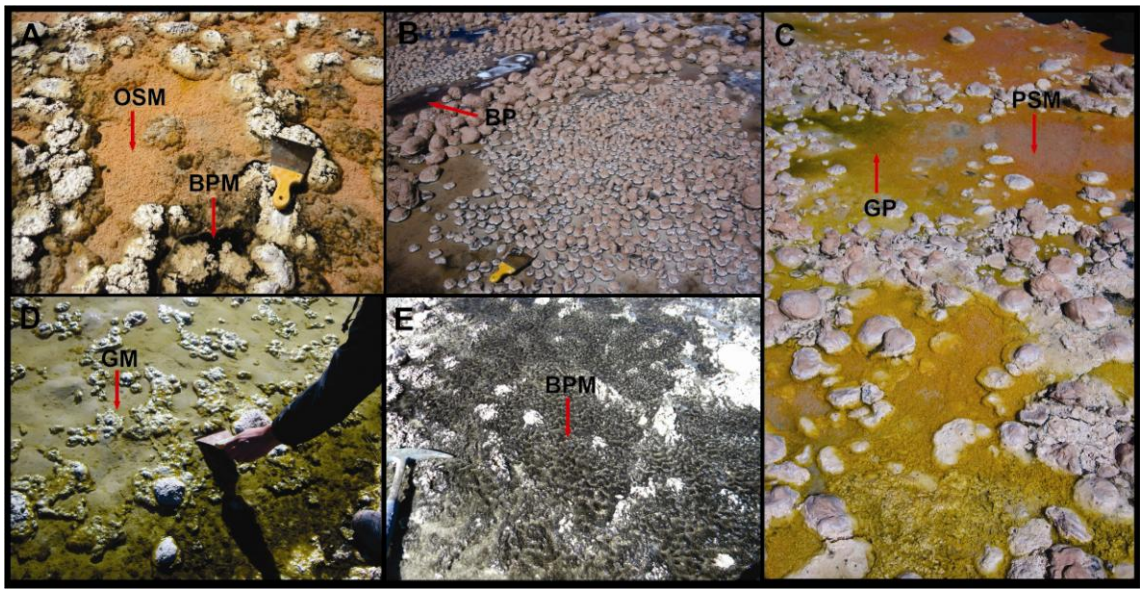

Figure 14.8 Different types of microbial mats found in the Stromatolite Belt area, associated with carbonates, mostly oncoids. **A)** Orange Stratified Mat (OSM), the most common microbial mat. Black Pustular Mat (BPM) is also observed surrounding partially exposed oncoids. **B)** Certain zones exhibit a blackish microbial community, here called Black Patch (BP). **C)** Pink Stratified Mat (PSM) near greenish patches (Green Patch-GP). **D)** A distinct microbial community develops a greenish soft bubble floating mat (Green Mat-GM) associated with insipient oncoids. **E)** Black Pustular Mat (BPM), a cyanobacterial dominated community that is located close to water-air interface covering carbonate crusts.

14.8 Microbial mats diversity

The LN system allows studying the relationship between microorganisms and calcium carbonate precipitation. As stated, the environmental conditions, like high UV exposure, high salinity, temperature fluctuations and strong winds, restrict life mostly to bacteria, archaea and unicellular eukaryotes. The LN mats consist of complex microbial communities that develop in the interface between sediment and water in the Stromatolite Belt. The presence of diatoms and bacteria-diatom-mineral aggregates represents the main component of the LN

microbial mats. Pennate and centric diatoms are observed; although pennates appear to be more abundant. Some of the diatom groups recognized by morphological microscopy observation include *Achnanthesbrevipes*, *Halamphora*sp., *Naviculas*p., *Surirella*sp., and *Striatula*sp. (Gomez *et al* 2018). The distinctive abundance of diatoms reported in other Andean lakes, suggests their role as the primary producers in these high-altitude microbialitic systems (Faríase*t al* 2013, 2014; Rasuke*t al* 2014, 2015).

There is a variety of microbial mats inhabiting the Stromatolite Belt, with recognizable macroscopic differences in superficial coloration and textural aspects (Figure 14.8). The following descriptions correspond to the most remarkable types of microbial mats found covering the sediments in the area, and their related bacterial diversity according to 16S rDNA 454 pyrosequencing analysis.

14.8.1 OSM (Orange Stratified Mat)

The oncoids of the Stromatolite Belt are mainly associated with this type of microbial mat. These mats have an orange surface and a granular texture, and shows a stratified internal structure controlled by light and redox gradients (Teske and Stahl 2002), as commonly seen in microbial mats in hypersaline settings. There is a distinguishable orange top layer (1-2 cm thick), followed by a purple layer (2-5 mm thick), then a thin green layer and a black anoxic horizon at the very bottom (several cm to dm thick). Among the studied mats from the LN, this has the highest diversity based on observed species and Shannon index, and the lowest Dominance and highest Equitability, meaning that the most prominent groups are more evenly distributed in the community composition than in other mats (Gomez *et al* 2018). The most abundant phylum is Proteobacteria (24%) (Figure 14.9), mostly Alphaproteobacteria and Deltaproteobacteria (Figure 14.10). The most frequent Gammaproteobacteria OTU (Operational Taxonomic Unit) matches with *Halochromatium* sp., a purple sulfur bacterium, and the most common OTU of Deltaproteobacteria matches with *Desulfobacula* sp., a marine sulfate-reducing bacterium with the capacity to degrade aromatic compounds. Other remarkable phyla found are Spirochaetes (14%), Verrucomicrobia (12%), Bacteroidetes (11%), and candidate phylum OD1 (currently named Parcubacteria, 10%) (Figure 14.9), whose members were recently described as probably being ectosymbionts or parasites of other organisms (Nelson and Stegen 2015).

14.8.2 PSM (Pink Stratified Mat)

This mat presents a more pinkish coloration in the surface, a stratified internal structure, and a less granular texture. Bacteroidetes (22%) is the dominant phylum (Figure 14.9). Proteobacteria is found second in abundance (19%) and most of it belonged to the Desulfobacteraceae family in the Deltaproteobacteria class (Figure 14.10). The phylum Spirochaetes is also present (14%). Deinococcus-Thermus (8%) and Firmicutes (4%) are less abundant. These results show that heterotrophic saccharolytic bacteria are the main bacterial families detected and mostly include: Rhodothermaceae (Park *et al* 2014), Spirochaetaceae (Karami*et al* 2014) and Deinococcaceae (Makarova *et al* 2007). The Chromatiales order (anoxygenic photosynthetic bacteria) that use hydrogen sulfide as electron donor and accumulate elemental sulfur in globules inside their cells (Imhoff 2014) are also detected in abundance within this mat (for more details see Gomez *et al* 2018).

14.8.3 GP (Green Patch)

This mat represents an isolated greenish patch in between the PSM with a less stratified structure. The most abundant phylum present is Deinococcus-Thermus (19%), follow by Proteobacteria (18%), OD1 (Parcubacteria, 14%), Spirochaetes (11%), and Verrucomicrobia (9%) (Figure 14.9). Among Proteobacteria, Rhodobacteraceae (3%) and Desulfobacteraceae (4%) are abundant. The green coloration of this mat could be explained by the abundance of diatoms, as the highest number of Stramenopiles chloroplast 16S rDNA sequences is recorded in this mat.

14.8.4 BP (Black Patch)

This is another patchy community, restricted to shallow ponds in between oncoids. The bacterial diversity record is clearly distinct. The BP had the lowest diversity with a lower Equitability and higher Dominance index in comparison with other spots and the stratified sites (Gomez *et al* 2018) (Figure 14.9). In this mat, half of the sequences belong to Firmicutes (53%), the dominant phylum. Within Firmicutes, nearly 44% of it belongs to *Halanaerobium* sp., Halanaerobiaceae (98% identity Greengenes database) (Figure 14.10). This genus may indicate the predominance of anaerobic fermentative halophilic communities. Other relatively abundant groups include Proteobacteria (11%), and Verrucomicrobia (6%).

14.8.5 GM (Green Mat)

This mat is observed closer to the groundwater springs, it is a green mat occasionally observed floating due to the presence of gas bubbles. The pyrosequencing analysis of the GM shows that most of the members belong to the Bacteroidetes phylum (30%) (Figure 14.9). Roughly 17% of them corresponds to the Saprospiraceae family (Figure 14.10), which is known to have an important role in the breakdown of complex organic compounds (McIlroy and Nielsen 2014). Besides, Flavobacteriaceae (11%) (Figure 14.10), mostly *Winogradskyella* sp. is detected. Verrucomicrobia is abundant as well with a representation of 26%. Proteobacteria is well represented with 18%, where an 83% of the relative abundance in this group belongs to Alphaproteobacteria (mostly Rhodobacteraceae). In comparison with all the others mats, the phylum Deinococcus-Thermus is not observed within the GM.

14.8.6 BPM (Black Pustular Mat)

There are clear macroscopic characteristics that make this mat unique. Cyanobacterial colonies develop a pustular to pinacular surface built by filaments, and it has a distinct black coloration that might be due to the scytonemin pigment from the cyanobacteria for protection against UV radiation. The BPM is commonly found in shallow ponds (a few cm) near the coast of the lake, close to the water-air interface, or colonizing the rims of partially exposed oncoids. This mat presents the highest Dominance index, and the lowest Equitability, meaning that the taxonomic groups present have uneven relative abundances and that only few of them dominate the community (Gomez *et al* 2018). The 37% of the bacterial diversity belongs to Deinococcus-Thermus (all Deinococcaceae family), Verrucomicrobia (17%) with families like Spartobacteriaceae (10%) and Puniceicoccaceae (4%), and Proteobacteria (10%), mainly Alphaproteobacteria (4%, with Rhodobacteraceae and Rhodospirillaceae members) and Gammaproteobacteria (3%) (Figure 14.9). Remarkably, in terms of diversity, the BPM is the only type of microbial mat in the LN that presents a significant abundance of the phylum Cyanobacteria (11%), mainly Rivulariaceae (10,5%) (Figure 14.10). Most groups present in the mat are heterotrophic bacteria, except for Cyanobacteria, and the most

abundant family (Deinococcaceae) includes saccharolytic bacteria (Makarova *et al* 2007), probably able to degrade EPS (Extracellular Polymeric Substances) produced by diatoms.

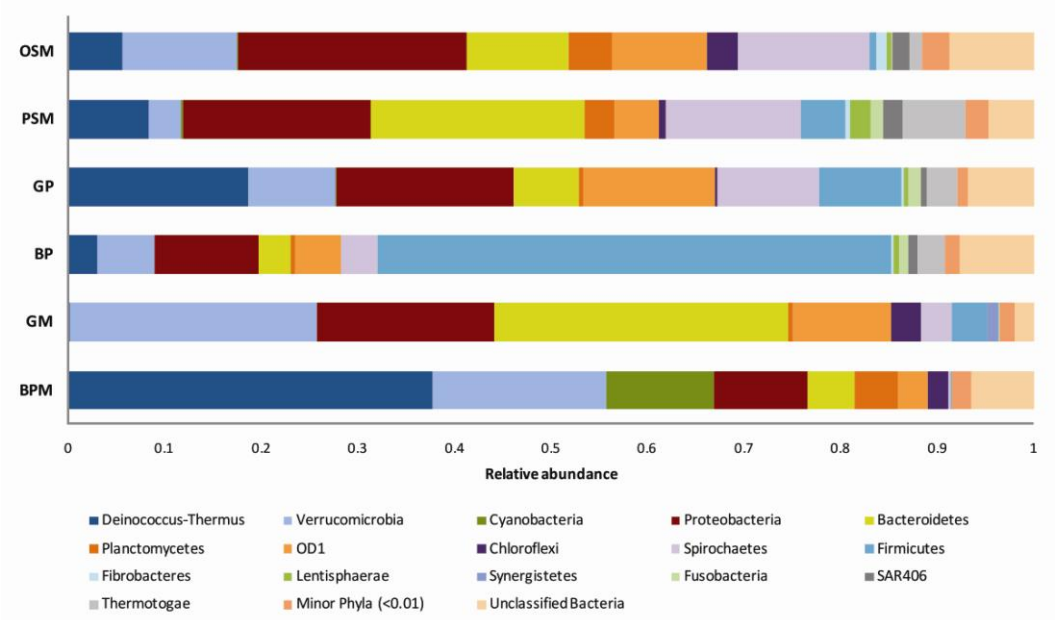

Figure 14.9 Relative abundance of phylum-level bacterial composition derived from each type of microbial mat sampled. Note Deinococcus-Thermus, Verrucomicrobia, Proteobacteria, Bacteroidetes, Spirochaetes and Firmicutes among the most representative phyla in almost all samples studied. Category "Minor Phyla (<0.01)" includes classified phyla present in less than 1% relative abundance: Acidobacteria, Actinobacteria, Armatinmonadetes, Chlamydiae, Chlorobi, Gemmatimonadetes, and Tenericutes.

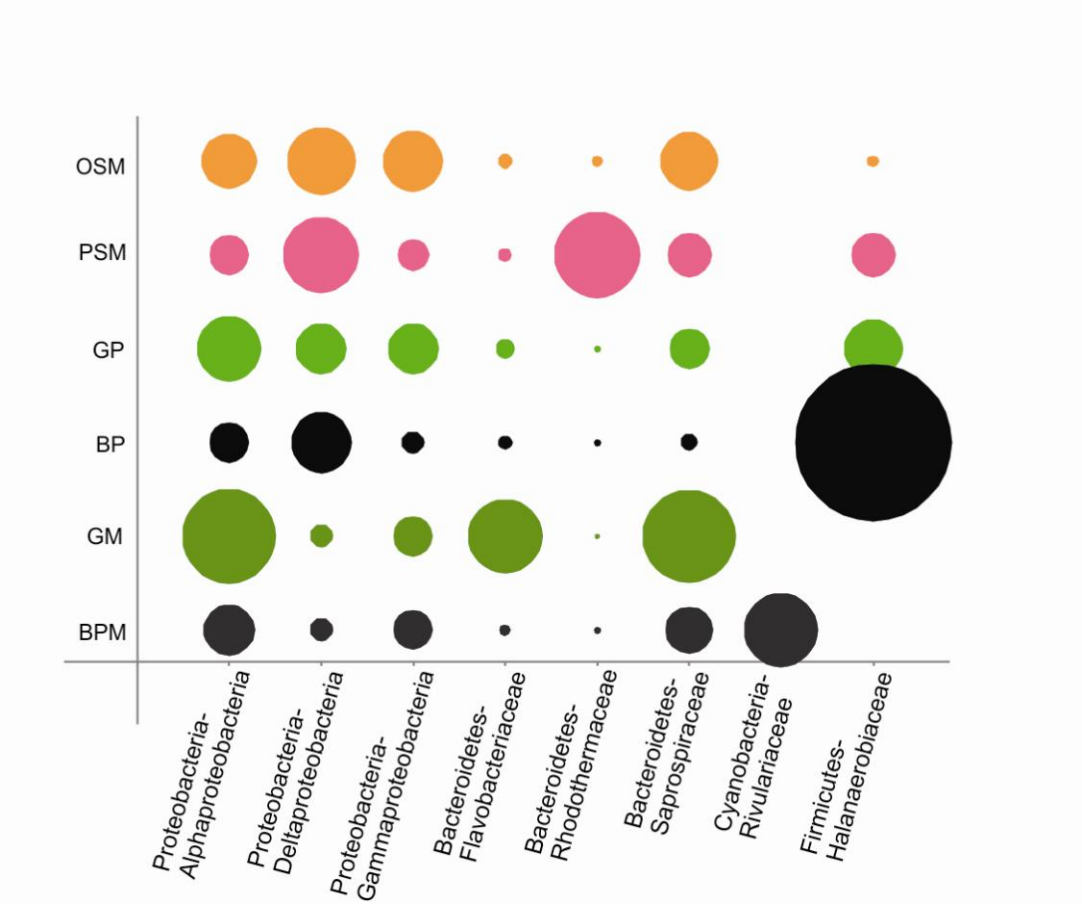

Figure 14.10 Relative abundance of most remarkable subphylum level groups in each microbial mat sampled.

In summary, considering all the different mats, the diversity analysis shows that Proteobacteria, Verrucomicrobia, Bacteroidetes and Deinococcus-Thermus are the most representative phyla in almost all samples studied. Other phyla like Spirochaetes and the gram positive Firmicutes are also abundant. All these groups are well known to be abundant in marine ecosystems and also in extreme environments, such as microbial mats from hypersaline systems like Shark bay (Wong *et al* 2015), Abu Dhabi (Abed *et al* 2008), Guerrero Negro (Harris *et al* 2013) among others; with few differences like the absence of Acidobacteria and Actinobacteria phyla. The LN microbial community seems to be similar at the phyla level with other Andean ecosystems, known as High Altitude Andean Lakes (HAALs). Deinococcus-Thermus is a group of bacteria known for their high UV radiation tolerance (Ivanova *et al* 2011), and is also recorded in other HAALs like Tebenquiche, La Brava (Faría*set al* 2014, Fernandez *et al* 2016), Socompa (Faría*set al* 2013, Toneatti*et al* 2017), Diamante (Rascovan*et al* 2016), Cejar, Llamara, Jachucoposa, and Pujsa (Rasuk*et al* 2016), where the UV radiation is one of the environmental challenges that organisms have to cope with. Cyanobacteria is one of the major groups in the BPM but is lesser represented or absent in the rest of the mats sampled in the LN and in other HAALs. However, confocal microscopy observations detected the presence of cyanobacteria in all analyzed samples from the LN, although not as a dominant group (Gomez *et al* 2018). This distinction of the BPM is also reflected in PCoA analysis, where the BPM does not cluster with any other bacterial community studied. Something similar occurs with the non-stratified GM; this mat appears distant in the analysis, remarking differences in the taxonomical composition of the community (Figure 14.11).

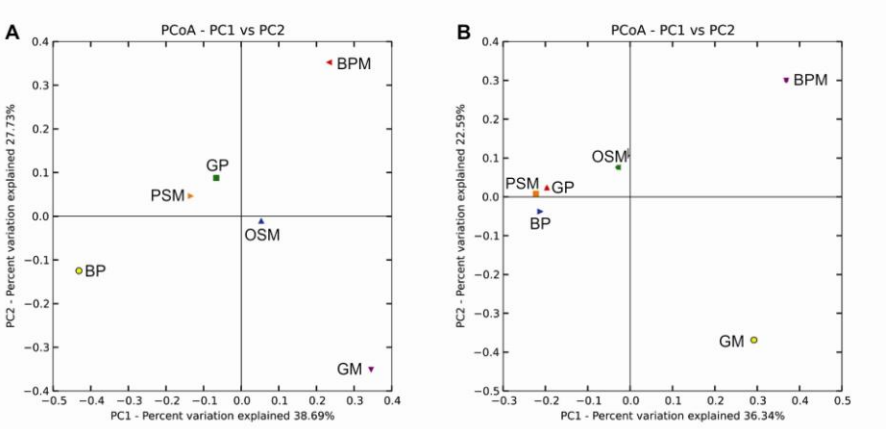

Figure 14.11 Bacterial communities clustered using PCoA of the weighted **(A)** and unweighted **(B)**UniFrac distance matrices. Each point corresponds to a different microbial mat sampled. The percentages of variation explained by the plotted principal coordinates are indicated on the axes.

To better characterize the BPM, the predominant filamentous cyanobacterium was collected, isolated and culture for a 16S-23S ITS phylogenetic and morphological characterization. The isolated strain presents unambiguous morphological characteristics, such as wider trichomes and filaments, uniquely branched trichomes, and mucilaginous pads at the bases of young trichomes. Additionally, based on the molecular phylogenetic analysis, the strain was found to be a unique and an independent lineage on the evolutionary tree belonging to the genus *Rivularia* inside the Rivulariaceae family (Shalygin*et al* 2018). As a result, considering the morphological and phylogenetic analyses, the cyanobacterial strain retrieved from the LN constitutes a new species (see Shalygin*et al* 2018 for details) under requirements of the International Code of Nomenclature for Algae, Fungi and Plants, named ***Rivularia halophila* sp. nov.**(Figure 14.12). It worth mentioning that *Rivularia halophila* is

the first species of the *Rivularia* genus reported from inland, hypersaline aquatic environment.

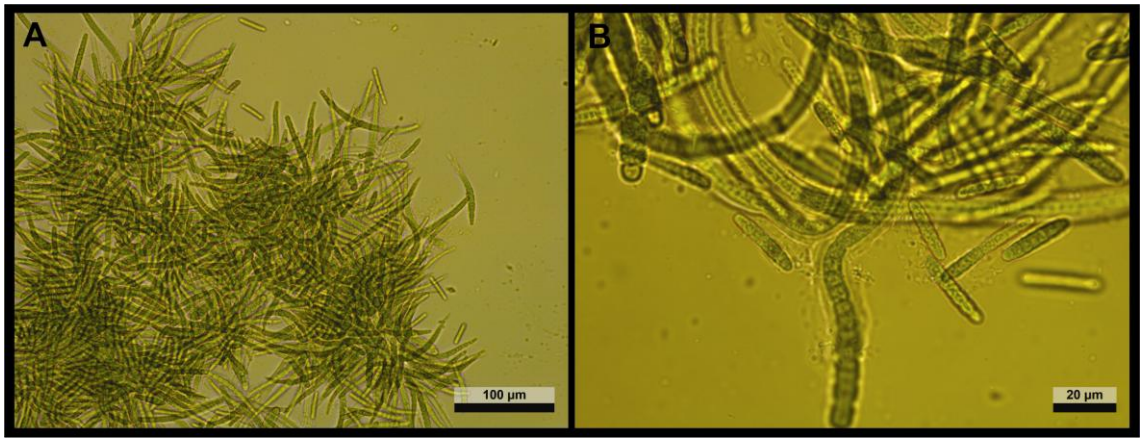

Figure 14.12 Microscopy photographs of *Rivularia halophila*, the representative cyanobacterium of the BPM. **A)** Almost spherical colonies, with radial arrangement of filaments. **B)** Detail of filaments, where short juvenile stages are visible.

Different types of carbonate laminae are identified within the oncoids and these seem to be partly associated with different microbial communities (for details see Gomez *et al* 2014, 2018). Interestingly, laminae with calcified *Rivularia*-like cyanobacterial filaments showing tufted palisade fabrics are observed alternating with micritic and botryoidal laminae (see details in Table 1). Gomez *et al* (2018) and Mlewski*et al* (2018) showed that carbonate precipitation is not directly associated with *Rivularia* itself (sheats are not usually calcified) but with the microbial consortia living around the *Rivularia* filaments, where diatoms and anoxygenic phototrophic bacteria are particularly abundant (for details see Mlewski*et al* 2018). This is interesting given the fact that *Rivularia*-like filaments have been observed in the fossil stromatolite record, so this may have implications to better understand *Rivularia* mineralization and preservation. For this, a more detailed study focused on the microorganisms belonging to the consortia existing around the *Rivularia Halophila* filament was conducted (Mlewski*et al* 2018).

Phylogenetic analyses (by Sanger sequencing) on the bulk BPM and whole genome amplificationon laser microdissected filaments highlighted the presence of Bacteroidetes affiliated to *Marivirga*(Pagani *et al* 2011), *Maribacter* and *Winogradskyella*. All these genera constitute the most abundant epiphytic bacterial community associated with the *Rivularia* filaments (Mlewski*et al* 2018). Proteobacteria and Verrucomicrobia are also among the most abundant phyla detected. Interestingly, members of Gammaproteobacteria found here, have their closest relative uncultivated bacteria (98% identity) retrieved from the Altiplano at Salar de Ascotan in Chile.

Interestingly, *Rivularia halophila*does not present any carbonate precipitation on their sheath itself. The microorganisms located on the cyanobacterial sheath may metabolically modify the local physico-chemical conditions and induce or preclude carbonate precipitation.The analysis of the microorganisms specifically associated to *Rivularia halophila* sheaths revealed that these are affiliated to epiphytic members of Bacteroidetes phylum, more specifically to the *Maribacter* genus that includes heterotrophic bacteria (Nedashkovskaya*et al* 2004). Thus, their activity possibly induces acidic conditions by producing CO_2 around the *Rivularia* sheaths, precluding carbonate precipitation (Dupraz and Visscher 2005,Dupraz*et al* 2009) and explaining in part, the absence of carbonation on the *Rivularia halophila* sheaths.

As previously stated, carbonate precipitation typically occurs on the EPS matrix around the *Rivularia* filaments and not on the sheaths (Mlewski*et al* 2018) and this may have implications to better understand taphonomic aspects of cyanobacteria calcification in the rock record. EPS-related carbonate precipitation was also observed in all described LN mats, within the EPS matrix excreted by a diverse diatoms-bacterial consortium (Gomez *et al* 2018, Mlewski*et al* 2018). Diatoms and other microorganisms such as Myxococcales and methanogenic archaea are known to produce large amounts of EPS (Baptiste*et al* 2005, Scholten *et al* 2005). These EPS should serve as nucleation sites for carbonate precipitation following organo-mineralization. In addition to the photosynthetic activity of *Rivularia* (for the BPM case) and diatoms that promoted local alkalinization, some other bacteria identified in the whole microbial community potentially present metabolisms that favors carbonate precipitation. For example, some bacteria belonging to the Myxococcales order are known to favor mineral precipitation (Jimenez-López *et al* 2007) by ammonification, enhancing the alkalinity of the medium (González-Muñoz *et al* 2010). Besides, some of the aerobic anoxygenic phototrophic bacteria (AAnPB) affiliated to the marine Roseobacter clade are known to interact with marine phytoplankton, including diatoms and this association allow microbes to use metabolic niches that would be inaccessible otherwise (Overmann and van Gemerden 2000,Schink 2002, Orphan *et al* 2008). Most of the members of the Roseobacterclade are ureolysers and some are denitrifiers (Luo and Moran 2014). Both ureolysis (Zhu and Dittrich 2016) and denitrification metabolisms (Ersan*et al* 2015) increase pH in the surrounding medium and favor carbonate precipitation. Hence, phototrophy, ureolysis and denitrification associated with the activity of AAnPB may be important drivers of alkalinization and carbonate precipitation in the BPM.

14.10 Concluding remarks

Carbonate precipitation is expected to occur in the LN, given that mixing between groundwater springs (alkalinity-rich) and the main lake waters (calcium-rich) increase saturation state triggering carbonate precipitation (Gomez *et al* 2014). In addition to mixing, other physico-chemical processes like evaporation and strong CO_2 degassing also contribute to increase saturation states, thus promoting carbonate precipitation (Beeler *et al* in press,see also Gomez *et al* 2019, this volume). Despite this, the extensive microbial mat system also contributes, through its metabolic activity, to carbonate precipitation. This occurs by changing chemical equilibrium (producing alkalinity) and providing nucleation sites for mineral precipitation, particularly due to the presence of EPS. This is recorded in the carbonate micro-textures in the oncoids and stromatolites as well as in the microbial mats (Table 1). Some of the recognized microbes show metabolisms that potentially contribute to carbonate precipitation including sulfate reduction, ammonification, oxygenic and anoxygenic phototrophic bacteria, uroelyzers and denitrifiers (Gomez *et al* 2018, Mlewski*et al* 2018). This microbial influence has an impact on the texture of the microbial carbonates, which is evident when comparing laminar crusts (where no microbial matsare visible), oncoids and stromatolites (where microbial mats and biofilms are present). By using carbon and oxygen isotope proxies the LN carbonates have also proven to be useful to record local environmental changes (Gomez *et al* 2014, Buongiorno *et al* 2018). These include variable mixing rates of groundwaters and lake waters, strong CO_2 degassing and evaporation as well as regional environmental changes, for example, the progressive increase in moisture and *freshening* of lake waters is related to recent climate changes. Unraveling the relative influences of these different controls in carbonate precipitation, micro-textures and geochemical signatures is challenging, even in these modern active systems, so care must be taken when working in the rock record. Thus, a combined multiproxy approach in modern

systems like the LN provides some insights to better understand the biosphere-geosphere interactions and record in modern and ancient systems.

14.11 References

Abed, R. M. M., Kohls, K., Schoon, R., Scherf, A.K., Schacht, M., Palinska, K.A., Al-Hassani, H., Hamza, W., Rullkötter, J. and Golubic, S. (2008). Lipid biomarkers, pigments and cyanobacterial diversity of microbial mats across intertidal flats of the arid coast of the Arabian Gulf (Abu Dhabi, UAE). *FEMS Microbiology Ecology 65*, (3):449-462. https://doi.org/10.1111/j.1574-6941.2008.00537.x

Arp, G., Reimer, A. and Reitner, J. (2001). Photosynthesis-induced biofilm calcification and calcium concentrations in the Phanerozoic oceans. *Science 292*, 1701-1704.

Allwood, A., Walter, M.R., Kamber, B.S., Marshall, C.P. and Burch, I.W. (2006). Stromatolite reef from the Early Archaean era of Australia, *Nature 441*, 714-718.

Awramik, S.M. and Buchheim, H.P. (2009). A giant, late Archean lake system: the Meentheena Member (Tumbiana Formation; Fortescue Group), Western Australia. *Precambrian Research 174*, 215-240.

Baker, E. and Beaudoin, Y. (2013). SPC, Deep Sea Minerals: Manganese Nodules, a physical, biological, environmental, and technical review. In Baker, E. and Beaudoin, Y. (Eds.), Vol. 1B, Secretariat of the Pacific Community.

Bapteste, E., Brochier, C. and Boucher, Y. (2005). Higher-level classification of the Archaea: evolution of methanogenesis and methanogens. *Archaea 1*, 353-363. doi: 10.1155/2005/859728

Beeler, S., Gomez, F. J., Bradley, A. in press. Controls of extreme isotopic enrichment inmodernmicrobialites and associated abiogenic carbonates, *GeochimicaetCosmochimica Acta*.

Buick, R.(1992). The antiquity of oxygenic photosynthesis: evidences from stromatolites in sulphate-deficient Archean lakes. *Science 255*, 74-77.

Buongiorno, J., Gomez, F. J., Fike, D., Kah, L.C. (2018). Mineralized microbialites as archives of environmental evolution, Laguna Negra, Catamarca Province, Argentina. *Geobiology1*,1-24.

Burne, R. and Moore, L. (1987). Microbialites: organo-sedimentary deposits of benthic microbial communities. *Palaios2*, 241-254.

Dupraz, C. and Visscher, P. T. (2005). Microbial lithification in marine stromatolites and hypersaline mats. *Trends Microbiol. 13*, 429-438. doi: 10.1016/j.tim.2005.07.008

Dupraz, C., Reid, R. P., Braissant, O., Decho, A. W., Norman, R. S. and Visscher, P. T. (2009). Processes of carbonate precipitation in modern microbial mats. *Earth Sci. Rev. 96*, 141-152. doi: 10.1016/j.earscirev.2008.10.005

Erşan, Y. Ç., de Belie, N. and Boon, N. (2015). Microbially induced $CaCO_3$ precipitation through denitrification: an optimization study in minimal nutrient environment. *Biochem. Engineer. J. 101*, 108-118. doi: 10.1016/j.bej.2015.05.006

Farías, M. E., Contreras, M., Rasuk, M. C., Kurth, D., Flores, M. R., Poiré, D. G., Novoa, F. and Visscher, P. T. (2014). Characterization of bacterial diversity associated with microbial mats, gypsum evaporites and carbonate microbialites in thalassic wetlands: Tebenquiche and La Brava, Salar de Atacama, Chile. *Extremophiles 18*, 311-329. https://doi.org/10.1007/s00792-013-0617-6

Farías, M. E., Rascovan, N., Toneatti, D. M., Albarracín, V. H., Flores, M. R., et al. (2013). The Discovery of Stromatolites Developing at 3570 m above Sea Level in a High-Altitude

Volcanic Lake Socompa, Argentinean Andes. *PLoSOne 8*, (1):e53497. https://doi.org/10.1371/journal.pone.0053497

Fernandez, A. B., Rasuk, M. C., Visscher, P. T., Contreras, M., Novoa, F., Poire, D. G., Patterson, M. M., Ventosa, A. and Farías, M. E. (2016). Microbial Diversity in Sediment Ecosystems (Evaporites Domes, Microbial Mats, and Crusts) of Hypersaline Laguna Tebenquiche, Salar de Atacama, Chile. *Frontiers in Microbiology 7*, 1284. doi: 10.3389/fmicb.2016.01284.

Gomez, F.J., Boidi, F.J., Mlewski, C. and Gerard, E. (2019). The carbonate system in hypersaline lakes: The Laguna Negra case (Puna of Catamarca, Argentina). In: Farias, M.E. (Ed.),*Microbial ecosystems in Puna environments:biofilms, microbial matsmicrobialites and endoevaporites*(Chapter 19). Springer Books.

Gomez, F. J., Kah, L. C., Bartley, J. and Astini, R. A. (2014). Microbialites in a High-Altitude Andean Lake: multiple controls in carbonate precipitation and lamina accretion. *Palaios 29*, 233-249.

Gomez, F. J., Mlewski, C., Boidi, F. J., Farías, M. E. and Gérard, E. (2018). Calcium Carbonate Precipitation in Diatom-rich Microbial Mats: The Laguna Negra Hypersaline Lake, Catamarca, Argentina. *Journal of Sedimentary Research 88*, (6):727-742. https://doi.org/10.2110/jsr.2018.37

González-Muñoz, M. T., Rodriguez-Navarro, C., Martínez-Ruiz, F., Arias, J. M., Merroun, M. L. and Rodriguez-Gallego, M. (2010). Bacterial biomineralization: new insights from Myxococcus-induced mineral precipitation. In Pedley, H. M. and Rogerson, M. (Eds.), *Tufas and Speleothems: Unravelling the Microbial and Physical Controls*, Vol. 336 (pp. 31-50). London: Geological Society; Special Publications.

Harris, J. K., Caporaso, J. G., Walker, J. J., Spear, J. R., Gold, N. J., Robertson, C. E., Hugenholtz, P., Goodrich, J., McDonald, D., Knights, D., Marshall, P., Tufo, H., Knight, R. and Pace, N. R. (2013). Phylogenetic stratigraphy in the Guerrero Negro hypersaline microbial mat. *The ISME Journal 7*, 50-60. https://doi.org/10.1038/ismej.2012.79.

Hawkins, C., Angheluta, L., Hammer, Ø. and Jamtveit, B. (2013). Precipitation dendrites in channel flow. *EPL 102*, doi: 10.1209/0295-5075/102/54001.

Hawkins, C., Angheluta, L., Hammer, Ø. (2004). Hydrodynamic shadowing effect during precipitation of dendrites in channel flow. *Physical Review, E 89*, 022402.

Imhoff, J. F. (2014). International Committee on Systematics of Prokaryotes Subcommittee on the taxonomy of phototrophic bacteria: minutes of the closed online meeting. *Int J SystEvolMicrobiol 64*, 3910-2. doi: 10.1099/ijs.0.068908-0

Ivanova, N., Rohde, C., Munk, C., Nolan, M., Lucas, S., Del Rio, T. G. et al. (2011). Complete genome sequence of *Trueperaradiovictrix* type strain (RQ-24 T). *Stand GenomicSci 4*, 91-99. doi: 10.4056/sigs.1563919

Jimenez-López, C., Jroundi, F., Rodriguez-Gallego, M., Arias, J. M. and González- Muñoz, M. T. (2007). Biomineralization induced by Myxobacteria. In Méndez-Vilas, A (Ed.), *Communicating Current Research and Educational Topics and Trends in Applied Microbiology*, Vol. 1 (pp. 143-154). Badajoz: Formatex.

Kang, C. H., Han, S. H., Shin, Y., Oh, S. J. and So, J. S. (2014). Bioremediation of Cd by microbially induced calcite precipitation. *Appl. Biochem. Biotechnol. 172*, 2907-2915. doi: 10.1007/s12010-014-0737-1

Karami, A., Sarshar, M., Ranjbar, R., Sorourizanjani, R. (2014). The Phylum Spirochaetaceae. In Rosenberg, E., Delong, E. F., Lory, S., Stackebrandt, E., and Thompson, F. (Eds.), *The Prokaryotes* (pp. 915-929). Berlin, Heidelberg: Springer.

Kwak, M. J., Lee, J. S., Lee, K. C., Kim, K. K., Eom, M. K., Kim, B. K. et al. (2014). *Sulfitobactergeojensis* sp. nov., *Sulfitobacternoctilucae* sp. nov., and

Sulfitobacternoctilucicola sp. nov., isolated from coastal seawater. *Int. J. Syst. Evol. Microbiol. 64*, 3760-3767. doi: 10.1099/ijs.0.065961-0

Lucena, T., Ruvira, M. A., Macián, M. C., Pujalte, M. J. and Arahal, D. R. (2013). Description of *Tropicibactermediterraneus* sp. nov. and *Tropicibacterlitoreus* sp. nov.*Syst. Appl. Microbiol. 36*, 325-329. doi: 10.1016/j.syapm.2013.04.001

Luo, H. and Moran, M. A. (2014). Evolutionary ecology of the marine Roseobacter clade. *Microbiol. Mol. Biol. Rev. 78*, 573-587. doi: 10.1128/MMBR.00020-14

Makarova, K. S., Omelchenko, M. V., Gaidamakova, E. K., Matrosova, V. Y., Vasilenko, A. et al. (2007). *Deinococcusgeothermalis*: the pool of extreme radiation resistance genes shrinks. *PLoS One 26*, e955.

Mlewski, E. C., Pisapia, C., Gomez, F., Lecourt, L., Soto Rueda, E., Benzerara, K., Ménez, B., Borensztajn, S., Jamme, F., Réfrégiers, M. and Gérard, E. (2018). Characterization of Pustular Mats and Related *Rivularia*-Rich Laminations in Oncoids From the Laguna Negra Lake (Argentina). *Frontiers in Microbiology 9,* 996. DOI=10.3389/fmicb.2018.00996.

Nedashkovskaya, O., Kim, S., Kyun Han, S., Lysenko, A. M., Rohde, M., Rhee, M. S. et al. (2004). *Maribacter* gen. nov., a new member of the family Flavobacteriaceae, isolated from marine habitats, containing the species *Maribactersedimenticola* sp. nov., *Maribacteraquivivus* sp. nov., *Maribacterorientalis* sp. nov. and *Maribacterulvicola* sp. nov.*Int. J. Syst. Evol. Microbiol. 54*, 1017-1023. doi: 10.1099/ijs.0.02849-0

Nedashkovskaya, O., Vancanney, T., Seung, B. and Zhukova, N. (2009). *Winogradskyellaechinorum* sp. nov., a marine bacterium of the family Flavobacteriaceae isolated from the sea urchin *Strongylocentrotus intermedius*. *Int. J. Syst. Evol. Microbiol. 59*, 1465-1468. doi: 10.1099/ijs.0.005421-0

Nelson, W. C. and Stegen, J. C. (2015). The reduced genomes of Parcubacteria (OD1) contain signatures of a symbiotic lifestyle. *Frontiers in Microbiology 6*, 713.

Orphan, V. J., Jahnke, L. L., Embaye, T., Turk, K. A., Pernthaler, A., Summons, R. E. et al. (2008). Characterization and spatial distribution of methanogens and methanogenic biosignatures in hypersaline microbial mats of Baja California. *Geobiology 6*, 376-393. doi: 10.1111/j.1472-4669.2008.00166.x

Overmann, J. and van Gemerden, H. (2000). Microbial interactions involving sulfur bacteria: implications for the ecology and evolution of bacterial communities. *FEMS Microbiol. Rev. 24*, 591-599. doi: 10.1111/j.1574-6976.2000.tb00560.x

Pagani, I., Chertkov, O., Lapidus, A., Lucas, S., Del Rio, T. G., Tice, H. et al. (2011). Complete genome sequence of *Marivirgatractuosa* type strain (H-43). *Stand. Genomic Sci. 4*, 154-162. doi: 10.4056/sigs.1623941

Park, S., Akira, Y. and Kogure, K. (2014). The family Rhodothermaceae. In Rosenberg, E., Delong, E. F., Lory, S., Stackebrandt, E. and Thompson, F. (Eds.), *The Prokaryotes* (pp. 849-856). Berlin, Heidelberg: Springer.

Rascovan, N., Maldonado, J., Vazquez, M. P. and Farías, M. E. (2016). Metagenomic study of red biofilms from Diamante Lake reveals ancient arsenic bioenergetics in haloarchaea. *The ISME Journal 10*, 299-309.

Rasuk, M. C., Fernandez, A. B., Kurth, D., Contreras, M., Novoa, F., Poiré, D. andFarías, M. E. (2015). Bacterial diversity in microbial mats and sediments from the Atacama Desert. *Microbial Ecology 71*, 44-56. doi: 10.1007/s00248-015-0649-9

Rasuk, M. C., Fernández, A. B., Kurth, D., Contreras, M., Novoa, F., Poiré, D. and Farías, M. E. (2016). Bacterial Diversity in Microbial Mats and Sediments from the Atacama Desert. *Microbial Ecology 71*, 44-56. https://doi.org/10.1007/s00248-015-0649-9

Rasuk, M. C., Kurth, D., Flores, M. R., Contreras, M., Novoa, F., Poire, D. and Farías, M. E. (2014). Microbial Characterization of Microbial Ecosystems Associated to Evaporites

Domes of Gypsum in Salar de Llamara in Atacama Desert. *Microbial Ecology 68*, 483-494.

Reitner, J., Paul, J., Arp, G. andHause-Reitner, D. (1996). Lake Thetis domal microbialites. Acomplex framework of calcified biofilms and organomicrites (Cervantes, Western Australia), in Global and Regional Controls on Biogenic Sedimentation. InReitner, J., Neuweiler, F. and Gunkel, F. (Eds.), *Reef Evolution Research Reports, Vol. SB2* (pp. 85–89). Göttingen: Göttinger Arb. Geol. Paläont, Sonderband

Schink, B. (2002). Synergistic interactions in the microbial world. *Antonie Van Leeuwenhoek 81*, 257-261.doi: 10.1023/A:1020579004534

Scholten, J. C. M., Joye, S. B., Hollibaugh, J. T. and Murrell, J. C. (2005). Molecular analysis of the sulfate reducing and archaeal community in a meromictic soda lake (Mono Lake, California) by targeting 16S rRNA, mcrA, apsA, and dsrAB genes. *Microbial. Ecol. 50*, 29-39. doi: 10.1007/s00248-004-0085-8

Shalygin, S., Pietrasiak, N., Gomez, F., Mlewski, C., Gerard, E. and Johansen, J. R. (2018). *Rivularia halophila* sp. nov. (Nostocales, Cyanobacteria): the first species of *Rivularia* described with the modern polyphasic approach. *European Journal of Phycology 53*, 537-548. doi: 10.1080/09670262.2018.1479887

Talbot, M.R. (1990). A review of paleohydrological interpretation of carbon and oxygen isotopic ratios in primary lacustrine carbonates. *Chemical Geology (Isotope Section)80*, 261-279.

Teske, A. and Stahl, D. A. (2002). Microbial mats and biofilms: evolution, structure and function of fixed microbial communities. In Staley, J. T. and Reysenbach, A. L. (Eds.) *Biodiversity of Microbial Life* (pp. 49-100). New York: Wiley-Liss, Inc.

Toneatti, D. M., Albarracín, V. H., Flores, M. R., Polerecky, L. and Farías, M. E. (2017). Stratified Bacterial Diversity along Physico-chemical Gradients in High-Altitude Modern Stromatolites. *Frontiers in Microbiology 8*, 646. doi: 10.3389/fmicb.2017.00646

Valero-Garces, B.L., Delgado-Huertas, A., Ratto, N. and Navas, A. (1999). Large 13C enrichment in primary carbonate from Andean Altiplano lakes, northwest Argentina. *Earth and Planetary Science Letters 171*, 253-266.

Valero-Garces, B.L., Delgado-Huertas, A., Ratto, N., Navas, A. and Edwards, L. (2000). Paleohydrology of Andean saline lakes from sedimentological and isotopic records, Northwestern Argentina. *Journal of Paleolimnology 24*, 343-359.

Visscher, P. and Stolz, J. (2005). Microbial mats as bioreactors: populations, processes and products. *Palaeogeography, Palaeoclimatology, Palaeoecology 219*, 97-100.

Wong, H. L., Smith, D. L., Visscher, P. T. and Burns, B. P. (2015). Niche differentiation of bacterial communities at a millimetre scale in Shark Bay microbial mats. *Scientific Reports 5*, 15607. doi: 10.1038/srep15607

Zhu, T. and Dittrich, M. (2016). Carbonate precipitation through microbial activities in natural environment, and their potential in biotechnology: a review. *Front. Bioeng. Biotechnol. 4*, 4. doi: 10.3389/fbioe.2016.00004.